Chemical Physics Impact 7 (2023) 100371

Contents lists available at ScienceDirect

Chemical Physics Impact

journal homepage: www.sciencedirect.com/journal/chemical-physics-impact

Biocompatibility of ionic liquid tagged terpyridine complexes with potent biological activity

M. Antilin Princela [a,d], B.T. Delma [a,d], S. Lizy Roselet [a,d], M. Shirly Treasa [a,d], M. Jaya Brabha [b,d], C. Isac Sobana Raj [c,d,*]

[a] Department of Chemistry, Holy Cross College (Autonomous), Nagercoil-629004, Tamil Nadu, India
[b] Department of Chemistry, Annai Velankanni College, Tholayavattam, Tamil Nadu 629157, India
[c] Department of Chemistry and Research Centre, Nesamony Memorial Christian College, Marthandam. Tamil Nadu 629165, India
[d] Affiliated to Manonmaniam Sundaranar University, Abishekapatti, Tirunelveli 627012, Tamil Nadu, India

ARTICLE INFO

Keywords:
Terpyridine
Ionic liquids
Antimicrobial activity
Antioxidant activity
Anticancer activity

ABSTRACT

The current work deals with the study of novel and bioactive ionic liquid tagged terpyridine ligand and their complexes were synthesized using first row transition metal ions. The synthesized IL tagged complexes were characterized by UV, FT-IR, ^{1}H NMR, ^{13}C NMR, HRMS spectroscopic studies and also the structure of the complexes was confirmed by its spectral data. Moreover, the antibacterial, antifungal, antioxidant and anticancer studies were carried out to exhibit the bioactivity of the complexes. The antimicrobial studies of newly synthesized complexes were tested against five bacterial and two fungal strains by disc diffusion method. The iron complexes of terpyridine shows outstanding activity than the reference with zone of inhibition of 22-32 mm against the evaluated microorganisms. Furthermore, the antioxidant activity of the terpyridine complexes was assessed by phosphomolybdenum and NO radical scavenging assay. The reducing power of the synthesized complexes has shown potent antioxidant activity than the standard. Especially, Cu-tpy-IL and Zn-ttpy-IL have shown good radical scavenging activity exhibits an IC_{50} value of 42.45 and 40.85 μg/mL respectively. In addition, the anticancer activity of the complexes was analyzed by SRB assay. The report suggested that the complexes of Cu-ttpy-IL and Zn-ttpy-IL exhibiting prominent role in anticancer activity against HeLa and HT-29 cell lines possessing a GI_{50} value of <10 μg/mL. The obtained results revealed that the bioactive synthesized complexes could be used as a derivative in the field of drug inventions.

1. Introduction

Metal ions and its complexes were served as a key material in biological processes and it is responsible for various biological reactions in our daily life [1]. Metal complexes have a peculiar property to exist as multiple oxidation states, generating additional coordination site, increasing the reaction kinetics, altering the ligand affinity and mimicking the metalloenzymes and so on. Because of these properties, metals can easily bind with oxygen, sulphur and nitrogen atoms, which is present in the amino acids in DNA [2–4]. The recent trends in bioinorganic chemistry are to synthesize thermodynamically stable and kinetically labile, low-cost eco-friendly metal complexes [5] and to utilize these complexes for various biological targets especially for cancer treatment. Generally, the metal atom has a tendency like readily losing an electron from the outermost orbit and it existed as a cation, hence metal containing biomolecules (Haemoglobin) carry the oxygen throughout the body. Since metal atom is electron deficient in nature, it exists in variable oxidation states based on the environment [6]. This tendency attracts electron rich biomolecules like DNA and proteins. Due to this peculiar property, metal complexes induce electron shuttling between biomolecules and metal complexes.

In addition to this, many metal ions are responsible for natural evolution and biological functions. Practically, haemoglobin is an iron containing allosteric protein which is present in blood and it carries oxygen as well as carbon dioxide [7]. Calcium and its compounds are present in bones; hence it decides the skeletal system [8]. Ceruloplasmin is the copper carrying protein made in liver, it stores and carries the mineral copper around our body [9]. Vitamin B-12 (cobalamin) is a cobalt containing vitamin, their contribution in the formation of red blood cell is a remarkable one [10]. Urease is a nickel containing

* Corresponding author.
E-mail address: isacchemistry@gmail.com (C.I.S. Raj).

https://doi.org/10.1016/j.chphi.2023.100371
Received 2 June 2023; Received in revised form 5 October 2023; Accepted 5 November 2023
Available online 7 November 2023

metalloenzymes, which hydrolyse urea into carbon dioxide and ammonia in large intestine [11]. Carboxypeptidase is zinc containing metalloenzymes which is crucial for many processes in the human body including digestion, blood clotting, and reproduction [12]. Considering this wide scope of metal complex in biological system, we planned to mimic the enzymes and metalloproteins by our IL tagged terpyridine based complexes.

From 19th century, terpyridine holds a sound record in the field of science and engineering. Terpyridine possess admirable structural orientation in space, excellent chelating ability towards transition metals, easy and convenient method of preparation, biocompatibility with biomolecules, highly conjugated flexible structures, superior thermal and mechanical stability and maintaining the multiple redox nature at lowest potential [13,14]. Therefore, terpyridine was utilized in emerging research fields like photochemistry [15,16], adsorption studies [17,18], energy storage devices [19,20], sensors [21,22], catalysis [23,24], biological applications [25,26], core material for dendrimer synthesis [27], precursors in nanoparticle synthesis [28,29], fluorescence studies [30,31], water oxidation and CO_2 reduction reactions [32,33]. Though terpyridine complexes have been used in various fields, their role in medicinal chemistry is crucial. Especially terpyridine complexes proficiently intercalates with base pair of the nucleic acids. Hence it is effectively used as an excellent anticancer drug. Moreover, based on the strong literature report we found that, protein and enzyme molecules were having metal binding sites like cysteine, histidine, and selenocysteine. Hence, terpyridine metal complexes and their bioisosteres binds with biomolecules easily and exhibits robust antiproliferative activity against malignant cells. And also, terpyridine complexes have a power to inhibit the metalloproteinase matrix that inhibits the activity of topoisomerase I, and topoisomerase II via ligand exchange reaction with the enzymes [34]. All these efforts increased the efficiency and easy delivery of metal complexes to the specified biological targets.

In addition to that, tridentate semicyclic terpyridine based ligands were very famous for the coordination of first row transition elements. Since, this terpyridine ligands have wide surface area with high conjugation system, it results in admirable biostability, excellent biocompatibility and intermolecular π-π stacking interaction with biomolecules persuades to utilize this ligand and their complexes in the field of coordination as well as medicinal chemistry [35]. Generally, terpyridine complexes have excellent intercalative binding nature with biomolecules. This is because of the easy accommodation of aromatic polypyridyl planar ring into the base pair of the DNA structure. Due to this, terpyridine complexes act as a best pharmacophore by easily intercalating with DNAs yielding metallodrugs towards the targeted cells. This peculiar intercalating properties influence the biological and medical activities of terpyridine complexes. Thus, this special way of non-covalent stacking mode of interactions with the double helical structures leads more attention on terpyridine systems towards pharmacological applications [36].

While considering the biological role of terpyridine coordinated metal complexes, here in we recounted the reported works have been published in the literature. Ezhilarasu et.al reported the symmetrical and unsymmetrical Ru (II)-bis(terpyridine) complexes derived from 4'-functionalized 2,2':6',2''-terpyridine possesses potent antibacterial activity. In addition, the antifungal performance of the aforementioned Ru (II) complexes showing appreciable results against Candida albicans [37]. Further, the Cu (II) complexes of 4′-(3-Methoxyphenyl)-2,2′:6′-2″-terpyridine, 4′-(4-methoxyphenyl)-2,2′:6′-2″-terpyridine and 4′-(3,5-dimethoxyphenyl)-2,2′:6′-2″-terpyridine were demonstrated as better anticancer activity against HeLa cell lines than cis-platin was reported by Liang et. al [38]. Chelate complexes of Cu (II) and Ni (II) attached with terpyridine ligand containing multiple aromatic rings exhibiting good activity against the evaluated bacterial strains [39]. Furthermore, Cu (II) and Zn (II) complexes derived from lipoic acid conjugated terpyridine as ligand was synthesized and their cytotoxicity nature was investigated for breast and cervical cancer cells. Among that, copper complex displayed to be analogous anticancer potential as compared to cisplatin and also responsible for inhibiting the cell growth through apoptosis by Velugula et. al [40]. Naseri and his coworkers reported the complexes of Cr (III), Mn (II), Fe (III), Co (II), Ni (II), Cu (II) and Zn (II) tagged with the ligand 4'-(2-thienyl)-2,2';6',2''-terpyridine (thioterpy). Particularly, Cr (II), Cu (II) and Zn (II) complexes demonstrating significant activity towards the assessed microrganisms. Besides this, the above stated complexes were subjected to check the anticancer activity on K562 cell lines, murine lung fibrosarcoma L929 and murine bone marrow cells (control). The observed findings explained that the synthesized complexes exhibiting better inhibitory action against the tested cell lines. Moreover, Mn (II) complex of thioterpy ligand acts a best superoxide radical scavenger than the natural enzyme [41]. Recently we reported the biological activity of Fe, Co, Ni, Cu and Zn complexes of salen functionalized ionic liquids [42].

Ionic liquids (ILs) are the most prestigious new class of molecule in the world. ILs composed of entirely ions, because of weak Vander Waals interaction which exists as salts in a liquid form [43,44]. Generally, ILs considered as organic salts and also having ions with poorly coordinated, hence it exists as liquids at a low temperature [45]. The properties of the ILs can be tuned by the suitable choice of cation and anion. ILs have peculiar properties like tuneable viscosity, negligible vapour pressure, extremely high conductivity, high potential window, high electrical stability, high thermal stability. Because of these extraordinary properties, currently ILs have attracted an increasing interest in several areas such as energy storage devices, fuels, lubricants, pharmaceuticals, drug delivery, adsorption, fuel cell, electrolyte fabrication, electrode preparation catalyst in organic conversions, reducing the over potential in electrocatalytic reaction, organic medium in high thermal reaction, chromatographic techniques and so on [46–48]. In addition, numerous materials like activated carbon [49], mesoporous carbon [50], graphene oxide [51], montmorillonite [52] to remove the impurities in the contaminated water samples. Similarly, ILs have a tendency to capture all the molecule towards its surface and hence it is used as a best adsorbent. However, it adsorbs all the drugs and hold himself and it delivers when it reaches the required site in the body.

On the other hand, ILs (ionic liquids) are known to have easily dissociable materials, tunable functional behaviours like hydrophilic and hydrophobic, biocompatibility with enzymes and other biomolecules [53]. Since ILs exist as ionic in nature and terpyridine act as σ-bonded ligands with aromatic side arms, the IL tagged terpyridine complex involve in sandwich type intercalative interactions with adjacent base pairs of nucleic acids. In addition to that, IL tagged terpyridine complexes exhibit ionic and metallic character. Hence it readily binds with DNA and engender cell death within a short time. Thus, the tendency of direct metal coordination, flexible structure and σ-bond conjugated systems are responsible for the activity of our IL tagged terpyridine complex towards the targeted cells. Also, IL tagging with the ligand affects the function and nature of the complex, while implementing this context, their lipophilicity enormously increases which is a first criteria for designing a new drug. Several efforts were made to increase the biological activity of ionic liquids as well as metal complexes. But no attempts were made to showcase the biological activity by tagging the IL with metal complex as a single molecule. Since, benzimidazolium based ILs and ttpy complexes are the best pharmacophore, we had an idea to combine both the pharmacophores as a single one, to increase the biological activity. Hence, we intended to utilize them synergistically along with metal terpyridine complex for biological application. With this in mind, we have synthesized ionic liquid tagged metal terpyridine complexes and explored their potential biological activity towards targeted cell lines.

In the current study, we synthesized the terpyridine tagged IL and its five new complexes of Fe, Co, Ni, Cu and Zn. The structure of the ligand and complexes were analyzed by UV-Visible, IR, NMR and HRMS spectroscopic techniques. Further, the antibacterial action of those

ligand and complexes were assessed by five bacterial and two fungal strains. Moreover, the antioxidant and free radical scavenging ability of the complexes were analyzed by Phosphomolybdenum method and NO radical scavenging assay respectively. Anticancer activity of terpyridine tagged complexes was evaluated using three cell lines such as HeLa, HT-29 and MCF-7 cell lines by SRB assay which explores that Cu-ttpy and Zn-ttpy indicates good activity against HeLa and HT-29 cell lines.

2. Experiment

2.1. Synthetic route for the preparation of ttpy-IL complexes

The scheme for the synthesis of ttpy-IL tagged metal complexes as follows and it was shown in Fig. 1.

2.2. Synthesis of 4′-(p-tolyl)-2, 2′:6′, 2″-terpyridine (ttpy) (1)

2-Acetylpyridine (3.633 g, 30 mmol) was mixed with 4-methylbenzaldehyde (1.802 g, 15 mmol) in ethanol (50 mL). At the meantime, NaOH pellets (1.197 g, 30 mmol) and aqueous NH_3 solution (40 mL, 30 %) were thoroughly mixed with the above stirred solution. In order to get the complete conversion, the reaction was extended up to 24 h. Furthermore, the newly formed precipitate was separated by vacuum filtration. During the end of vacuum filtration, once again the precipitate was purified and recrystallized with ethanol which offers off white solid **(1)**. Yield: 1.776 g; 55 %. Melting point: 160°C. IR (ATR) (ν/cm^{-1}): 3047 (C-H) (alkyl), 1642 (C═C) (aromatic), 1581 (C=N) (pyridine ring), 1463 (C-C) (phenyl ring), 785 (C-H) (aromatic). ^{1}H NMR (400 MHz, $CDCl_3$) δ: 2.42 (s, 3H, -CH_3), 7.304-7.367 (m, 4H, ArH), 7.813-7.891(m, 4H, ArH), 8.656-8.676 (d, J =8 Hz, 2H, ArH), 8.725-8.735 (d, J =4 Hz, 4H, ArH). ^{13}C NMR (100 MHz, $CDCl_3$) δ: 21.29, 118.64, 121.38, 123.77, 127.17, 129.66, 135.50, 136.85, 139.10, 149.05, 149.98, 155.89, 156.39.

2.3. Synthesis of 4′-(p-bromomethylphenyl)-2, 2′:6′, 2″-terpyridine (Br-ttpy) (2)

4′-(p-tolyl)-2, 2′:6′, 2″-terpyridine (4.849 g, 15 mmol), *N*-bromosuccinimide (NBS, 3.203 g, 18 mmol) and *a, a*′-azoisobutyronitrile (AIBN, 0.2 g, 1.2 mmol) were mixed thoroughly with anhydrous carbon tetrachloride (40 mL). The resultant concoction was refluxed (80 °C) for 2 h. The unreacted residues were removed at hot condition by filtration under the reduced pressure. The remaining solvent was removed by slow evaporation technique at 50 °C using water bath. The product obtained **(2)** was pale yellow in colour and further, acetone was chosen as a suitable solvent for recrystallization, which offered white needles. Yield: 4.646 g; 77 %. Melting point: 136 °C. IR (ATR) (ν/cm^{-1}): 3053 (C-H) (alkyl), 1652 (C═C) (aromatic), 1583 (C=N) (pyridine ring), 1465 (C-C) (phenyl ring), 785 (C-H) (aromatic), 597 (C-Br). ^{1}H NMR (400 MHz, $CDCl_3$) δ: 4.815 (s, 2H, -CH_2-Br), 7.523-7.554 (m, 2H, ArH), 7.652-7.673 (d, J =8.4 Hz, 2H, ArH), 7.939-7.919 (d, 4H, ArH), 8.658-8.678 (d, J =8 Hz, 2H, CH=N), 8.762-8.773 (t, 4H, ArH). ^{13}C NMR (100 MHz, $CDCl_3$) δ: 33.82, 117.90, 120.99, 124.58, 127.23, 127.33, 130.28, 137.55, 139.38, 148.80, 149.26, 154.78, 155.62.

2.4. Synthesis of 4′-(1-ethylbenzimidazole-N-methylphenyl)-2, 2′:6′, 2″-terpyridine bromide (3)

5 mmol of 1-Ethylbenzimidazole (0.730 g) was taken with 5 mmol 4′-(phenyl-p-bromomethyl)-2, 2′:6′, 2″-terpyridine (2) (2.011 g) and dissolved in acetonitrile (50 mL) and transferred in an RB flask. The contents in the flask were allowed to stir continuously and refluxed to maintain a temperature at 80 °C for 2 days. The resulting hot mixture was cooled to ambient temperature subsequently occurring caddy white precipitate. The crude product was washed by acetonitrile till the clear white precipitate was appeared. Further, the above precipitate was washed with ethyl acetate and rinsed with diethyl ether. The final

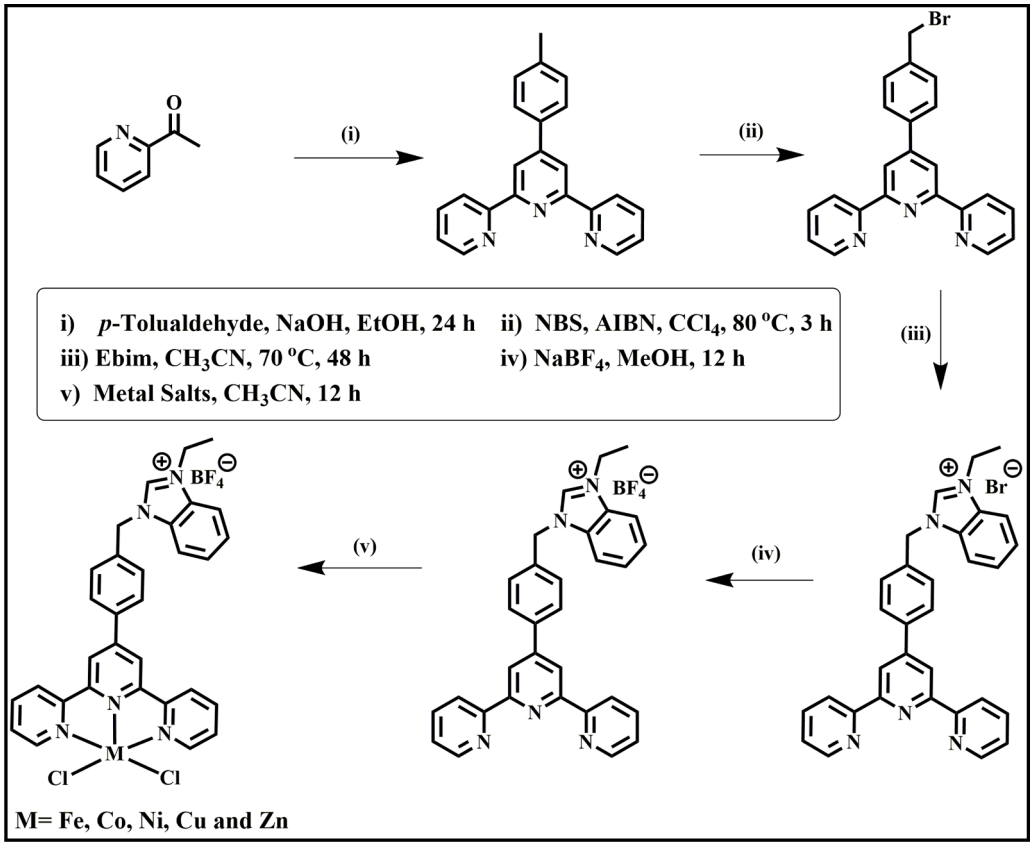

Fig. 1. Synthetic route of targeted ttpy-IL complexes.

product was heated at 50 °C in the forced-air circulating oven and dried. The shiny white crystalline precipitate **(3)**, 4′-(1-ethylbenzimidazole-N-methylphenyl)-2, 2′:6′, 2″-terpyridine bromide was obtained. Yield: 2.248 g; 82 %. Melting point: 212°C. IR (ATR) (ν/cm^{-1}): 3035, 1635, 1552, 1467, 1195 (quaternised nitrogen), 785 (C-H) (aromatic). ^{1}H NMR (400 MHz, DMSO-d_6) δ: 1.583-1.620 (t, J =7.6 Hz, 3H, -CH_3), 4.555-4.609 (q, J =7.2 Hz, 2H, -CH_2), 5.905 (s, 2H, Ph-CH_2-N), 7.520-7.553 (m, 2H, ArH), 7.663-7.694 (m, 4H, ArH), 7.701-7.767 (m, 6H, ArH), 8.660-8.693 (t, J =8 Hz, 4H, ArH), 8.747-8.757 (d, J =4 Hz, 2H, ArH), 10.045 (s, 1H, N-CH=N). ^{13}C NMR (100 MHz, DMSO-d_6) δ: 14.56, 42.77, 50.05, 114.37, 118.55, 121.48, 125.10, 127.13, 127.25, 128.10, 129.84, 131.45, 131.69, 135.70, 138.02, 138.43, 142.77, 149.38, 149.82, 155.32, 156.22.

2.5. Synthesis of 4'-(1-ethylbenzimidazole-N-methylphenyl)-2, 2':6', 2''-terpyridine tetrafluoro borate, (ttpy-IL) (4)

4′-(1-Ethylbenzimidazole-*N*-methylphenyl)-2, 2′:6′, 2″-terpyridine bromide (1.371 g, 2.5 mmol) was mixed with methanol (50 mL) and add slowly an aqueous tetrafluoroborate (0.272 g, 2.5 mmol) into the above solution. The contents in the reaction flask were stirred continuously at room temperature for 12 h. Once the reaction completed, the whole mixture was filtered by using Whatman filter paper 1 under reduced pressure. After filtering, the product was collected from the Porcelain Buchner Filtration Funnel as solid (4). White colour solid. Yield: 1.290 g; 93 %. Melting point: 126 °C. IR (ATR) (ν/cm^{-1}): 3080, 1656, 1564, 1467, 1205, 1058 (B-F), 769 (C-H) (aromatic). ^{1}H NMR (400 MHz, DMSO-d_6) δ: 1.581-1.617 (t, J =7.2 Hz, 3H, -CH_3), 4.548-4.602 (q, J =7.2 Hz, 2H, Ph-*CH_2-N), 5.886 (s, 2H, N-CH_2-), 7.525-7.555 (q, J =2 Hz, 2H, ArH), 7.686-7.755 (m, 4H, ArH), 7.991-8.140 (m, 6H, ArH), 8.667-8.700 (t, J =8 Hz, 4H, ArH), 8.750-8.761(d, J =4.4 Hz, 2H, ArH), 9.965 (s, 1H, N-CH=N). ^{13}C NMR (100 MHz, DMSO-d_6) δ: 14.55, 42.76, 50.05, 114.35, 118.56, 121.48, 125.11, 127.13, 127.26, 128.13, 129.31, 129.822, 131.46, 131.69, 135.69, 138.03, 138.45, 142.75, 149.38, 149.83, 155.31, 156.22. ^{19}F NMR (376 MHz, DMSO-d_6) δ: -148.25. UV-vis {λ_{max}, nm/ DMF}: 280 (π-π*). HRMS calcd for [$C_{31}H_{26}N_5$] [BF_4]; (M^+−BF_4) = 468.5690, found = 468.5688.

2.6. The common process for ttpy-IL complexes preparation

The solvent mixture methanol and acetonitrile (3:1) were chosen as the best solvents for the complexation reaction. This combined solvent mixture was used to dissolve the ttpy-IL ligand (4) (2. 5 mmol) effectively. Simultaneously, the metal salts (2.5 mmol) were dissolved in minimum quantity of methanol and added dropwise to the above-mentioned solution. In order to form the complex, the reaction was extended up to 12 h. Once the reaction completed, the crude product was filtered off, further it was recrystallized by methanol. It offers bright and attractive colourful complexes.

2.7. Synthesis of Fe-ttpy-IL complex (5)

According to the general procedure, IL attached terpyridine ligand (1.388 g, 2.5 mmol) was vigorously stirred with ferric chloride (0.4055 g, 2.5 mmol) suspension in methanol. Within 30 min yellowish brown precipitate was appeared in the reaction mixture. The reaction was extended up to 12 h to get higher yield. Then IL attached Fe-ttpy complex (5) was collected after filtration. Yield: 1.184 g, 67 %. Melting point: 242 °C. IR (ATR) (ν/cm^{-1}): 3068, 1608, 1562, 1481, 1192, 1022 (B-F), 794, 420 (Fe-N). UV-vis {λ_{max}, nm/ DMF}: 278 (π-π*), 575 (MLCT). HRMS calcd for [$C_{31}H_{26}Cl_3FeN_5$] [BF_4]; (M^+−BF_4) = 630.5770, found = 630.5773.

2.8. Synthesis of Co-ttpy-IL complex (6)

According to the general procedure with IL attached terpyridine as ligand (1.367 g, 2.5 mmol) was vigorously stirred with cobalt chloride (0.3245 g, 2.5 mmol) suspension in methanol. The reaction was extended up to 12 h. once the reaction completed, diethyl ether was added dropwise to the reaction mixture with constant stirring. The prepared complex (6) was generated as a pale green solid. Yield: 1.147 g, 67 %. Melting point: 266 °C. IR (ATR) (ν/cm^{-1}): 3066, 1604, 1566, 1471, 1197 (N^+-C) (quaternised nitrogen), 1060 (B-F), 790 (C-H) (aromatic), 428 (Co-N). UV-vis {λ_{max}, nm/ DMF}: 283 (π-π*), 327 (MLCT). HRMS calcd for [$C_{31}H_{26}Cl_2CoN_5$] [BF_4]; (M^+−BF_4) = 598.4081, found = 598.4079.

2.9. Synthesis of Ni-ttpy-IL complex (7)

According to the general procedure, 2.5 mmol of IL attached terpyridine as ligand (1.367 g) was added with 2.5 mmol of nickel chloride (0.3237 g) in minimum quantity of methanol. The complex (7) was precipitated and filtered. The precipitate was collected as an off white crystalline solid. Yield: 1.112 g, 65 %. Melting point: 282 °C. IR (ATR) (ν/cm^{-1}): 3091, 1606, 1566, 1475, 1195 (N^+-C) (quaternised nitrogen), 1051 (B-F), 792, 420 (Ni-N). UV-vis {λ_{max}, nm/ DMF}: 287 (π-π*), 330 (MLCT). HRMS calcd for [$C_{31}H_{26}Cl_2NiN_5$] [BF_4]; (M^+−BF_4) = 598.1684, found = 598.1681.

2.10. Synthesis of Cu-ttpy-IL complex (8)

According to the general procedure, an equimolar quantity of IL attached terpyridine as ligand (1.367 g) was added with the methanolic solution of copper chloride (0.336 g) in an RB flask. The precipitated green solids (8) were filtered and separates out. Yield: 1.1381 g, 66 %. Melting point: 212 °C. IR (ATR) (ν/cm^{-1}): 3001, 1606, 1554, 1475, 1195 (N^+-C) (quaternised nitrogen), 1066 (B-F), 790, 418 (Cu-N). UV-vis {λ_{max}, nm/ DMF}: 289 (π-π*), 348 (MLCT). HRMS calcd for [$C_{31}H_{26}Cl_2CuN_5$] [BF_4]; (M^+−BF_4) = 603.021, found = 603.0207.

2.11. Synthesis of Zn-ttpy-IL complex (9)

According to the general procedure, the same quantity of IL attached terpyridine as ligand (1.367 g) was mixed with dissolved zinc chloride (0.3407 g) in methanol. The formed complex (9) was precipitated as a white crystalline solid. Yield: 1.175 g, 68 %. Melting point: 288 °C. IR (ATR) (ν/cm^{-1}): 2978, 1600, 1566, 1475, 1199 (N^+-C) (quaternised nitrogen), 1055 (B-F), 794, 425 (Zn-N). UV-vis {λ_{max}, nm/ DMF}: 279 (π-π*), 342 (MLCT). HRMS calcd for [$C_{31}H_{26}Cl_2ZnN_5$] [BF_4]; (M^+−BF_4) = 604.855, found = 604.8548.

2.12. Evaluation of invitro antibacterial and antifungal activity

The prepared complexes of terpyridine tagged ionic liquids were assessed the antimicrobial and antifungal assay by using the standard protocol test procedure. Further, the disc was grown in petridish by spreading the Mueller-Hinton broth along with Sabouraud agar for aerobic and anaerobic bacterial strains [54]. Briefly, the nutrient broth was prepared by mixing 5 g peptic digest obtained from animal tissue, 1.5 g beef extract and 1.5 g yeast extract along with the addition of 5 g sodium chloride in 1 litre of water. The above broth solution was dissolved thoroughly. Moreover, the grown-up cells were picked from the stock culture with the help of micro streaker and it was loaded into the nutrient broth which was termed as inoculum. The inoculum was transferred in an Erlenmeyer flask and it was incubated at 37 °C for 72 h. Once the incubation was completed, the culture medium was turned into solid. Hence, the petri plates were loaded with inoculum while keeping the sterile swabs on bacterial suspension. Each terpyridine complex was dissolved with DMSO and it was diluted approximately with sterile water. 100 μL of ttpy-IL complex was added in each agar plate wells containing test organism. The sample loaded agar plates were incubated overnight at 37 °C for the colonial growth. After incubation, the growth

of microorganism on terpyridine complexes were calculated by means of zone of inhibition (in mm). The inhibition of microbial growth was determined by using the following strains like *B. subtilis* MTCC 5981, *S. aureus* MTCC 96 (Gram-positive bacteria), and *K. pneumonia* MTCC 3384, *P. aeruginosa* MTCC 424, *E. coli* MTCC 443 (Gram-negative organism) whereas the fungal strains such as *C. albicans* MTCC 227, *A. niger* MTCC 282. The standard drug used for the antimicrobial and antifungal study namely Amikacin and Nystatin respectively.

2.13. Antioxidant activity

2.13.1. General procedure for the anti-oxidant assay by phosphomolybdenum technique

The antioxidant nature of the synthesized ttpy-IL complexes to be analyzed by phosphomolybdenum assay [55]. 0.6 M sulphuric acid was added to a mixture of 28 mM sodium phosphate and 4 mM ammonium molybdate solution and it was taken as a reagent solution. Then, 1 mg/mL ttpy-IL complexes were added with 3.0 mL of reagent. Incubate the sample at 95 °C and it was allowed to cool at room temperature. Absorbance of the prepared complex was determined against blank solution. In addition, the blank was prepared by adding methanol (0.3 mL) instead of ttpy-IL complex and the same reagent 3.0 mL and further it was incubated at 95 °C. Ascorbic acid was used as a reference material. Therefore, the antioxidant ability was calculated in terms of number of gram equivalent of ascorbic acid.

2.13.2. Evaluation of NO radical scavenging ability

Nitric Oxide (i.e.) NO is an odd electron species and also diatomic in nature. It plays a crucial role in the immunity booster creates naturally in human body against microbial infections. Especially, NO possess less half-life period hence it could be oxidizing into nitrate as well as nitrite. In addition, nitric oxide act vigorously against pathogens which produces peroxynitrite (ONOO) and dinitrogen trioxide (N_2O_3). Moreover, microbes were highly affected by NO gas which leads to kill the microorganism effectively. At physiological pH, freshly prepared solution of aqueous sodium nitroprusside generates NO radicals. These radicals bind with oxygen to create nitrite ions. Griess reagent was used to analyze the amount of nitrite content. Griess reagent was prepared by an equimolar amount of 1 % sulphanilamide mixed with 2 % phosphoric acid and 0.1 % naphthyl ethylenediamine dihydrochloride [56].

In fact, ionic liquids have a tendency to scavenge nitric oxide radicals which could be realized as a promising and recovery medicine to cure the disorders. Moreover, nitric oxide scavengers undergo subsequent oxidation which leads to diminish the production of NO. In this scenario, NO radical scavenging ability of the synthesized ttpy-IL complexes were assessed by Griess reagent with the help of UV-visible spectrophotometer. Meanwhile, absorbance was recorded with and without the concentration of ttpy-IL complexes. Approximately taken the methanolic solution of ttpy-IL complex with constant concentrations (0-1000 μg/ml) and phosphate buffered saline solutions of sodium nitroprusside were mixed thoroughly and kept in a glass tube to maintain the pH at 7.5. Incubating the mixture at 30 °C under a visible polychromatic light for 3 h. Subsequently, the formed NO radical was combined with oxygen to produce nitrite ion. Alternatively, blank was performed in the absence of ttpy-IL complexes in addition to the same amount of buffer was used. Later, the concentration of nitrate ion was measured by diluting the half quantity of an incubation mixture with an equitable amount of the Griess reagent. Diazotization and Coupling reaction were done by sulphanilamide and naphthylethylenediamine- dihydrochloride with nitrite ions. Absorbance was recorded against blank solution in accordance with pink chromophore at 546 nm [57]. Each trail was accomplished in triplicate. Similar procedure to be followed to compare the methanolic solution of ttpy-IL complexes with standard ascorbic acid.

The inhibition percentage was calculated by the formula

$$\text{Percentage inhibition} = (\text{Optical density of Control} - \text{Optical density of Test} / \text{Optical density of control}) \times 100$$

2.14. Assessment of invitro Anticancer ability (SRB method)

The invitro anticancer activity of the synthesized ttpy-IL complexes were assessed against HeLa, HT-29 and MCF-7 cancer cell lines using SRB assay. To determine the cell proliferation activity of the complexes were described by the following standard protocol procedure. Initially, the cells were grown in culture by Roswell Park Memorial Institute (RPMI 1640) medium and cultivated it in the solution containing fetal bovine serum (10 %) along with L- glutamine (2 mM). In this experiment, 5×10^3 cells/ wells were seeded at a density of 100 μL in 96-well tissue culture microplates. Cells were stick on the plates to be incubated at 37 °C for 24 h which could be performed at a condition of 95 % air along with 100 % humidity and 5 % CO_2. In order to prepare the stock solution, synthesized ttpy-IL complexes were solubilized in DMSO at 100 mg/ mL and further it was diluted to 1mg/ mL with water. The mixture was stored and kept in refrigerator for further use. While the addition of ttpy-IL complex, 1 mg/mL of aliquot was thawed and diluted with different concentrations of 100, 200, 400 and 800 μg/mL. The above solution was transferred into the culture medium containing the test sample. Moreover, the ttpy-IL complexes were added with other dilutions of 10 μL aliquots which was introduced in the medium containing 90 μL in microtiter plates at a final concentration of ttpy-IL complexes i.e., 10, 20, 40 and 80 μg/mL [58].

Incubating the plates at 37 °C even after the addition of ttpy-IL complexes for 2 days and also the test was ceased by the addition of cold trichloroacetic acid. Simultaneously, cells were remained as such followed by the mild addition of cold solution of approximately 50 μL of 30 % trichloroacetic acid and kept in an incubator at 4 °C for 1 hr. Discard the supernatant liquid and the plates were washed several times with tap water and air-dried. Furthermore, 50 mL of 0.4 % SRB dye (Sulforhodamine B) mixed with 1 % (w/v) acetic acid was added in each well and the plates were placed in an incubator at RT for 20 minutes. Later the staining period, unbound dye was rescued and remove the residual dye through washing with 1 % (w/v) acetic acid, followed by the plates were air dried. Subsequently, the bound stain was washed with 10 mM trizma base. Adriyamycin was used as a positive control. The absorbance was recorded on a plate reader at a wavelength of 540 nm and a reference having 640 nm [59]. Each experiment was done as triplicate. After the 48 hrs of incubation, morphological changes were observed in cell culture and also the images of the cells treated under drugs to be captured by Phase Contrast Inverted Microscope along with digital camera system.

Growth percentage was determined on each plate of ttpy-IL complexes as correlated with the control wells. Growth percentage is defined as the total average of the absorbance of ttpy-IL complex to the absorbance observed in control wells x 100. From the absorbance data, growth percentage was measured for each concentration levels of the complexes. Growth percentage inhibition was found as:

$$\text{Percentage growth inhibition} = [\text{Ti}/\text{C}] \times 100\%$$

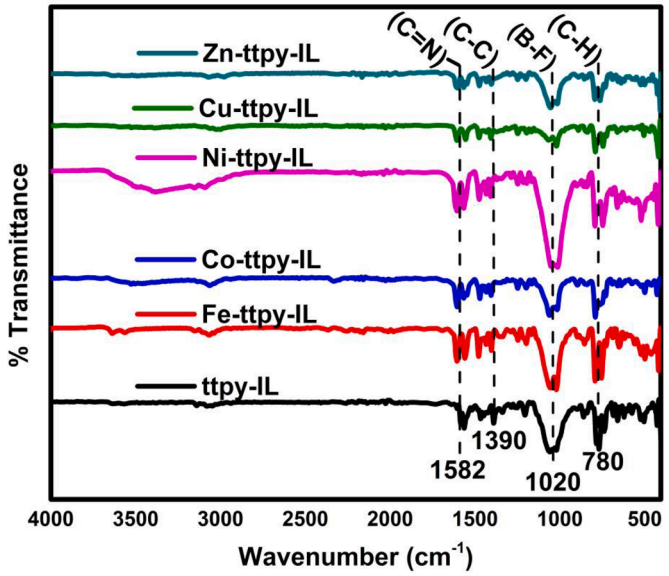

Fig. 2. FT-IR spectrums of ttpy -IL ligand and their complexes.

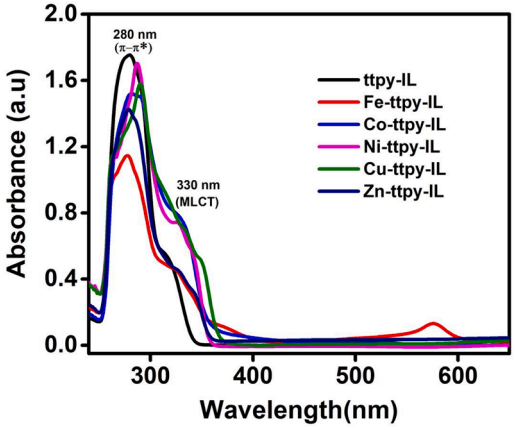

Fig. 3. UV-Visible spectra of ttpy-IL ligand and their complexes.

3. Results and discussion

3.1. Characterization of terpyridine ILs

The IL tagged terpyridine ligand and its complexes were successfully synthesized and analyzed using FT-IR, UV-visible, ^{1}H NMR, ^{13}C NMR & HRMS spectroscopic analysis.

The IR spectrum of ttpy-IL and its complexes were exhibited in the range of 4000-400 cm^{-1} and the obtained IR spectra were displayed in the Fig. 2. While stacking FT-IR spectra, the typical peaks for the ligand to be shifted more with respect to change in their intensities during the formation of the metal complex. In addition, the spectra of metal-ttpy-ILs were observed new characteristic vibrational peaks. The vibrational progressional spacings of ligand and its complexes were exhibited a peak at 2900-3100 cm-1 which was attributed to the C—H stretching of alkyl group present in the ligand [60]. The characteristic ν(C=N) in the terpyridine sphere was showed the peaks at 1560 cm^{-1} for ligand and 1600-1610 cm^{-1} for the complex [61].

Moreover, the absorption peak of ν(C=N) was enhanced in their energy due to the metal which could be coordinated with terpyridine. Notably, the former vibrational mode shows a slight shift of 40 cm^{-1} from the ligand, owing to the metal ion coordinated with the terpyridine nitrogen atom. Further, a sharp intense peak at 1390-1410 cm^{-1} corresponds to the ν (C=C) stretching for aromatic ring carbons present in the tridentate ttpy-ILs. Both the ligand and the complex were accompanied with the IL, as indicated by the bands at 1190 -1210 cm^{-1}, which could be attributed for quaternized nitrogen (N^{+}-C) and vibrational modes of alkylated N-methyl (CH_2-N) group at 1260 cm^{-1}. The vibrational frequency of ttpy-IL ligand & their complexes were exhibited an expansive peak at 1020-1060 cm^{-1} which was attributed for the uncoordinated tetrafluoroborate (B-F) anion, which confirms that, even after the complex formation there is no change in the position of tetrafluoroborate anion [62]. Furthermore, in terpyridine ligand there was no band observed less than 500 cm^{-1} whereas in complexes, the observed peaks at 420, 428, 420, 418 and 425 cm^{-1} correspond to metal- nitrogen (M-N) linkage for Fe, Co, Ni, Cu and Zn respectively [63].

The ligand and its metal complexes of terpyridine tagged ILs were analyzed, recorded using UV-vis absorption spectroscopy and the spectral data was shown in Fig. 3. DMSO was used as a solvent to dissolve the samples. UV-vis absorption spectra exhibit maximum intense peak at 280 nm on account of π→π* transitions in terpyridine ligand. In terpyridine tagged metal complexes showed absorption band at 575 nm for Fe-ttpy-IL, 327 nm for Co-ttpy-IL, 330 nm for Ni-ttpy-IL, 348 nm for Cu-ttpy-IL and 342 nm for nm for ttpy-IL owing to (MLCT) i.e., metal to ligand (d→π*) charge transfer in all complexes. Further, we noticed that Fe-ttpy-IL alone gives two absorption band. A high intense peak show at 327 nm resembles to a MLCT d→π* (χ) electronic transition, this is due to the electronic transition between higher energy π* symmetric orbital and metal d-orbital. While in lower frequency, a band arises at 560 nm assigned to the MLCT d→π* (ψ) transition, was due to the electronic transition between lower energy π* antisymmetric orbital and metal d-orbital [64].

^{1}H & ^{13}C NMR spectra of synthesized IL tagged terpyridine ligand was interpreted by using obtained data and displayed in supporting information. In ^{1}H NMR spectrum, the resonance frequency δ at 1.581-1.617 ppm appeared as triplet for the terminal methyl proton. The signal observed for methylene proton appeared in between the methyl group and benzimidazolium nitrogen exhibited as quartet with resonance δ at 4.548-4.602 ppm. The two protos present in N-CH_2 group appeared as a singlet in the region of δ 5.886 ppm which was linking terpyridine core unit and benzimidazolium moiety. In case of aromatic proton in terpyridine ligand, several signals were observed as quartet, multiplet and triplet with a range of δ 7.525-8.761 ppm [65]. An intense peak was noted at δ 9.965 ppm as singlet in downfield shift region due to the existence of (N-CH=N) group. ^{13}C NMR spectrum of IL tagged terpyridine ligand was depicted in supporting information. The resonate frequency at δ 14.55- 50.05 was corresponds to the aliphatic carbons present in the terpyridine ligand. Furthermore, the signals for aromatic carbons were showed the signals at δ 114.35- 156.22 ppm. In addition to that, there was an anion such as tetrafluoroborate in ligand ttpy-IL giving ^{19}F NMR resonance at δ -148.25 ppm.

The structures of the synthesized ttpy-IL and their complexes were deduced with the mass spectrum. It reveals that there was a noticeable change in the ttpy-IL ligand and its complexes by m/z values. The peak with m/z value at 468 assigned as a molecular ion peak of the fragment $[C_{31}H_{26}N_5]^{+}$. Meanwhile, the peak at m/z = 630.5773 confirmed the composition of $[C_{31}H_{26}Cl_3FeN_5]^{+}$ of Fe-ttpy-IL complex in the mass data. Accordingly, the prepared complex Co-ttpy-IL shows an ion peak m/z = 598.4079 confirmed the composition of $[C_{31}H_{26}Cl_2CoN_5]^{+}$ in the mass spectrum. Similarly, in Ni-ttpy-IL complex shows a band at m/z = 598.1681 provided as a molecular ion peak for the corresponding composition of $[C_{31}H_{26}Cl_2NiN_5]^{+}$. In the case of Cu-ttpy-IL complex, the mass spectrum exhibits a molecular ion peak with the m/z value of 603.0207 confirmed the composition of $[C_{31}H_{26}Cl_2CuN_5]^{+}$. Moreover, the Zn-ttpy IL complex displayed a band in the mass spectrum with m/z of 604.8548 which resembles the fragment $[C_{31}H_{26}Cl_2ZnN_5]^{+}$ and it would be employed as a molecular ion peak. Further, the base peak of

ttpy-IL ligand and their complexes showing the m/z value =146 assigned to the presence of ethyl benzimidazolium ion $[C_9H_{10}N_2]^+$ with the elimination of p-tolyl-terpyridine molecule. Finally, the aforementioned data giving the strong evidence towards the formation of proposed ligand and complexes.

3.2. Antimicrobial and antifungal assay

IL encapsulated terpyridine complexes of transition metals (Fe, Co, Ni, Cu & Zn) were evaluated against two-gram + ive bacteria such as Bacillus subtilis, Staphylococcus aureus and three gram -ive bacteria like K. pneumoniae, Pseudomonas aeruginosa, E. coli and also two fungi such as Candida albicans, Aspergillus niger.

The analysis of ILs with microbes of inhibition zones exposed that the terpyridine ligand and its complexes acquires magnificent activity for all the tested bacterial and fungal strains which was displayed in Fig. 4. An interesting finding was observed that Fe-ttpy complex exhibits admirable performance as compared to the reference amikacin for the aforementioned bacteria. It was reported from earlier literature, the activity of these complexes was due to the highly aromatic rigid nature of molecular structures and thus the complexes can able to form chelation [66].

Herein, we have analyzed the data from Table 1, the complexes exhibiting remarkable performance of all the tested bacterial & fungal microorganisms as compared with the control amikacin. Certainly, Fe and Cu complexes of terpyridine ILs demonstrated better efficacy against B. subtilis and S. aureus and also those complexes were active towards gram positive bacterial strains. Furthermore, in Klebsiella pneumoniae shows superior activity for the terpyridine ligand and also the complexes of Fe, Cu and Zn experiences activity than the standard. Fe-ttpy complex having good inhibition against Pseudomonas aeruginosa. Also, the ligand and its complexes of Fe and Ni tends to be active on E. coli. Therefore, the iron complexes of terpyridine shows outstanding activity against gram negative bacteria.

On the other hand, the antifungal activity of terpyridine ILs and its complexes had shown that Fe and Zn-ttpy complexes exhibits good activity against *Candida albicans* which was comparable with the standard. The analyzed complexes have shown moderate antifungal activity against Aspergillus niger but the iron complex could be marvelous in their activity. It is important to conclude that the enhanced antimicrobial activity of iron terpyridine IL complex was based on chelation theory. The positive charge of iron complexes may coordinate with lone pair of nitrogen on tridentate terpyridyl ligand that will decreases the polarity of the metal ion. This is because the sharing of pi-electron which is present in the donor atom as well as delocalization of pi-electron cloud on the chelate ring. Hence, this chelation augments the lipophilic nature of the corresponding complex which supports the permeability through the lipid layers of the cell membrane [67].

Generally, zinc atom is an inactive redox metal and it could be considered as redox inert species. Hence, Zn-ttpy complex showing less inhibitory action towards the assessed microbes. [68]. In addition, Cu (II) complexes have shown to be an antimicrobial agent which in turn

Table 1
Results of antibacterial and antimycotic activity of IL encapsulated terpyridine complexes.

Microorganism	Measurement of inhibition zones (mm)						
	ttpy - IL	Fe-ttpy-IL	Co-ttpy-IL	Ni-ttpy-IL	Cu-ttpy-IL	Zn-ttpy-IL	Amikacin/ Nystatin
B. subtilis	15	28	15	13	20	15	19
S. aureus	18	30	15	13	24	15	23
K. pneumonia	22	27	16	11	20	23	21
P. aeruginosa	15	26	14	12	15	14	22
E. coli	15	22	10	13	12	10	22
C. albicans	14	24	9	14	15	17	19
A. niger	**16**	32	10	11	15	11	18

effectively as free antibiotic. So, it has slight activity towards the positive strains [69]. Perhaps, the low antimicrobial performance of Ni (II) and Co (II) complex is due to the less solubility of the complexes as well as the pharmacophore is built by stable covalent bonds which could not be penetrate easily in the layers of bacterial lipid membrane [70]. However, chelation is not only responsible for antibacterial activity but also the activity depends on various factors such as dipole moment, geometry of the complex, solubility, nature and size of the metal ion and ligand, the redox potential of metal ion, steric hindrance and hydrophobicity. On the other hand, the permeability of the microbial cell wall giving preference in antibacterial activity which alters the ability of metal complexes [71]. Hence, the inhibitory mechanism of microbes may correlate with the findings.

3.3. Antioxidant activity of ttpy-IL complexes

The IL tagged terpyridine complexes tends to be active towards antibacterial and antimycotic activity. Hence, we had a desire to interpret the other biological strategies for the prepared complexes like antioxidant and antiproliferative activity. In order to extend the activity in research, we evaluated the reducing power of the IL tagged terpyridine complexes by phosphomolybdenum assay. Further, the radical scavenging effect of all the IL tagged terpyridine complexes were examined through nitric oxide assay. Incorporation of various metal center to the IL tagged terpyridine ligand does not shown any reducing power owing to the reduction of Mo^{6+} to Mo^{5+} was failed in the presence of (ttpy-IL) ligand as well as (metal-ttpy-IL) complexes. As a result, scientists have put greater effort into finding nontoxic antioxidants that could be effective NO radical inhibitors.

The current work reveals the scavenging of NO radical activity for all the IL tagged ttpy complexes were assessed by Nitric Oxide radical scavenging assay. The amount of scavenging power in percentage and 50 % growth inhibitory concentration values of all the IL tagged ttpy complexes were measured and shown in Table 2. At physiological pH, the IL tagged ttpy complexes demonstrated antioxidant potential in which the produced nitrite radicals from aqueous sodium nitroprusside were scavenged by the ILs imitating with oxygen. Especially, IL tagged

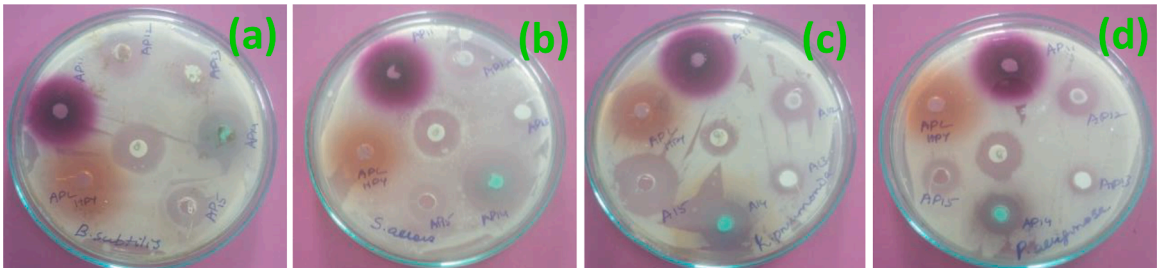

Fig. 4. Area of zones of inhibition images of antibacterial and antimycotic performance of IL tagged terpyridine complexes: (a) Bacillus subtilis, (b) Staphylococcus aureus, (c) Klebsiella pneumonia, (d) Pseudomonas aeruginosa, (e) Escherichia coli, (f) Candida albicans, (g) Aspergillus niger.

Table 2
NO radical scavenging activity (%) of dicationic ionic liquids.

Concentration (μg/ml)	Inhibitory activity (%)					
	Fe-ttpy-IL	Co-ttpy-IL	Ni-ttpy-IL	Cu-ttpy-IL	Zn-ttpy-IL	Ascorbic acid
25	52.95 ± 0.16	50.78 ± 0.51	40.86 ± 0.15	52.52 ± 0.64	43.26 ± 0.47	35.56 ± 0.01
50	47.69 ± 0.63	41.91 ± 0.71	35.13 ± 0.26	50.26 ± 0.71	49.00 ± 0.85	46.41 ± 0.27
100	44.52 ± 0.42	39.04 ± 0.49	34.95 ± 0.63	42.60 ± 0.29	51.00 ± 0.51	55.96 ± 0.73
250	28.69 ± 0.86	23.56 ± 0.62	39.47 ± 1.28	64.17 ± 0.25	68.26 ± 1.15	66.92 ± 0.15
500	22.08 ± 0.51	19.86 ± 0.39	41.91 ± 0.48	79.65 ± 0.46	78.95 ± 0.02	72.42 ± 0.36
800	28.56 ± 1.16	14.60 ± 0.83	42.95 ± 0.11	81.56 ± 0.29	78.49 ± 0.07	76.95 ± 0.73
IC_{50}	98.22 ± 0.41	>100	>100	42.45 ± 0.17	40.85 ± 0.38	89.67 ± 0.16

Data represented as Mean ± SD (n = 3).

copper and zinc complexes (Cu-ttpy-IL and Zn-ttpy-IL) can act as a free radical absorber and neutralizer, extinguishing the singlet and triplet states of oxygen, or decompose the peroxides [72]. The complexes of Cu and Zn possess high NO radical scavenging activity in association with low IC_{50} value denotes a higher NO radical inhibitory activity of Cu-ttpy-IL (IC_{50} = 42.45 μg/ mL), Zn-ttpy-IL (IC_{50} = 40.85 μg/ mL) and also it experiences promising antioxidant ability as compared to the standard ascorbic acid i.e., IC_{50} = 89.67 μg/ mL. The remaining complexes (Fe-ttpy-IL, Co-ttpy-IL and Ni-ttpy-IL) exhibiting higher IC_{50} values than compared with the standard ascorbic acid. Therefore, IL tagged iron, cobalt and nickel metal complexes were shown less antioxidant activity. As a result, Cu-ttpy-IL and Zn-ttpy-IL having more capability to inhibit the nitric oxide radicals and hence the two complexes could be recommended as a drug in the treatment for diseases [73].

The current investigation proves that, all the IL tagged ttpy complexes demonstrated the NO inhibition activity based on dose dependent manner. Even though, as we increase the concentration of IL tagged ttpy complexes would leads to increase the antioxidant potential and reaching a plateau. But in the case of iron, cobalt and nickel complexes, there is no gradual increment in the scavenging activity. However, Cu-ttpy-IL and Zn-ttpy-IL were showed marvelous NO radical scavenging ability than compared with the standard ascorbic acid. Therefore, benzimidazolium based IL tagged copper and zinc complexes muscularly expelled the nitrite radical even at low concentration in comparison with the other IL tagged ttpy complexes.

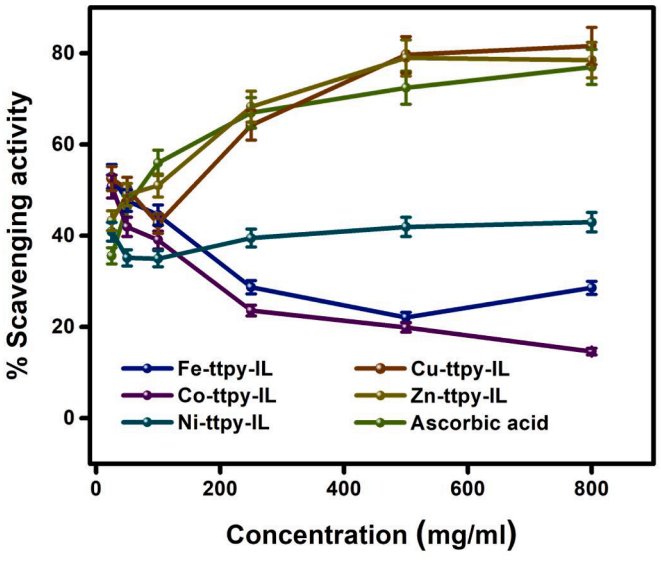

Fig. 5. In vitro free radical scavenging effect of IL tagged ttpy complexes by nitric oxide scavenging method.

In order to interpolate the free radical scavenging power and capability, the conclusion behind that, Cu-ttpy-IL has potent NO scavenging power at 800 μg/ml displayed in Fig. 5. Moreover, Cu-ttpy-IL and Zn-ttpy-IL were able to scavenge the NO radicals directly. Among that, Cu-ttpy-IL suppress the rapid NO generation and also have an ability to trap the NO with sodium nitroprusside in the biological medium at normal conditions. Owing to the electron or hydrogen donating tendency of copper and Zinc complexes, which leads to convert the reactive radicals into more stable and unreactive species. And also, it induced the quenching of NO radicals. Furthermore, Cu-ttpy-IL has a tendency to balance the unpaired electrons in which subsequently scavenging the free radicals and it leads to decrease the concentration of nitrite ions. These reports emphasize that, Cu-ttpy-IL has shown potent radical scavenging activity in correlation with the standard ascorbic acid.

3.4. Antiproliferative activity

Anticancer activity screening of IL attached terpyridine complexes were assessed by three cancer cell lines such as HeLa i.e., cervical cancer cell line, HT 29 i.e., colon carcinoma cell line and MCF-7 (breast carcinoma cell line).

Adriamycin was employed as a standard anticancer drug in SRB assay under the same conditions. Cell growth was examined by varying the concentration of IL tagged terpyridine complexes at constant intervals 10, 20, 40 and 80 μg/ml against % growth inhibition. The performance of IL attached terpyridine complexes was checked by GI_{50} values. The results obtained from SRB assay affirmed that, the antitumour assessment of IL tagged ttpy complexes against three different cell lines were displayed in Table 3. The GI_{50} values obtained by testing the affected cells on various concentrations of IL tagged terpyridine complexes suggested that the above mentioned (Table 3) concentration was required for inhibiting 50 % cell growth in the tested cell lines. It was also noted that the complexes having the GI_{50} value >80 μg/ml did not give an efficient cell death even at higher concentrations. Especially, the complexes of Co-ttpy IL, Cu-ttpy IL and Zn-ttpy IL have shown outstanding activity towards HeLa cell line when it was compared to the positive control.

In HT-29, Cu-ttpy IL and Zn-ttpy IL complexes possess better anticancer activity, whereas in MCF-7 cell line shown lowest activity on Fe-ttpy IL and Co-ttpy IL. The report indicated that, among the five IL tagged terpyridine complexes, the Cu-ttpy IL and Zn-ttpy IL complexes stimulates potent cell death on HeLa and HT-29 cell lines and also the Co-ttpy IL had exhibit an effective cell death on HeLa cell line with the GI_{50} value <10 μg/ml.

The invitro anticancer screening of IL tagged terpyridine complexes were noted and it was compared with the standard adriamycin in a dose dependent curve as displayed in Fig. 6. The dose dependent curve was drawn graphically by changing the IL concentration with percentage

Table 3
Anticancer activity of terpyridine ILs against human cancer cell lines.

Terpyridine ILs	50 % growth inhibition (μg/ml) *		
	HeLa	HT-29	MCF-7
Fe-ttpy IL	64.1	34.2	58.7
Co-ttpy IL	<10	>80	60.7
Ni-ttpy IL	>80	>80	>80
Cu-ttpy IL	<10	<10	>80
Zn-ttpy IL	<10	<10	>80
Adriamycin	<10	<10	<10

* GI_{50} shows the amount of terpyridine ILs consumed for 50 % of cell growth inhibition.

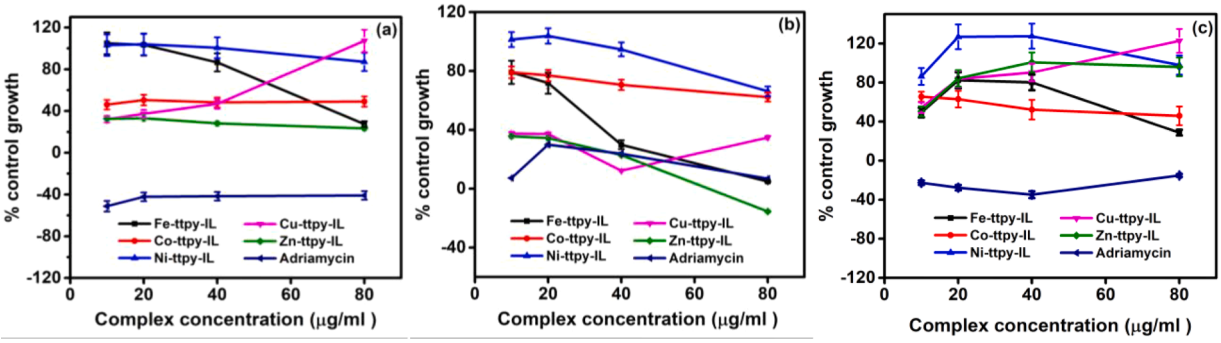

Fig. 6. Dose response curves of IL tagged ttpy complexes with reference adriamycin on HeLa (cervical), HT-29 (colon) and MCF-7 (breast) cancer cell lines.

growth of inhibition. The efficiency of IL tagged terpyridine complexes showed that, while increasing the complex concentration, there was a change in percentage control growth. In HeLa cell line (Fig. 6a) the complexes of Co, Cu and Zn were active towards Adriamycin. These complexes were attained the 50 % cell inhibition at low concentration (10 μg/ml) and maintained the constant level in control growth of cancer cells. Unexpectedly, copper complex was increased in their percentage control growth at maximum concentration (80 μg/ml). This may cause forbidding the destruction of cancer cells by the copper complex in HeLa cell line. Moreover, in HT-29 cell line (Fig. 6b) the complexes of Fe, Cu and Zn having potent anticancer activity against cancer cells. Further, Fe-ttpy IL reveals significant anticancer activity on HeLa (cervical cancer), HT-29 (colon cancer) and MCF-7 (breast cancer) cell lines exhibiting the GI_{50} value as 64.1, 34.2 and 58.7 μg/ml respectively.

The active complexes of terpyridine reached 50 % growth inhibition at minimum concentration whereas the remaining two complexes were inactive because it did not achieve the 50 % inhibition even at maximum concentration. Similarly, the Zn-ttpy IL brings the enhanced activity towards the increasing concentration of complex more than that of the control adriamycin. Also, the Fe-ttpy IL attained the 50 % inhibition at 40 μg/ml and further decreases its GI_{50} value, thus would increase the percentage growth inhibition. In Cu-ttpy IL, the percentage growth inhibition was reached less than 50 % at initial ttpy-IL concentration i.e., 10 μg/ml, but the control growth ratio was increased at higher concentrations (upto 80 μg/ml). In the context of MCF-7 breast cancer cell line (Fig. 6c), there was no significant activity of IL tagged terpyridine complexes may correlate with the positive control.

All the complexes had given the percentage growth inhibition above 50 % at even minimum concentration. At higher concentrations, Fe-ttpy IL and Co-ttpy IL exhibits the GI_{50} value 58.7 and 60.7 μg/ml respectively, which was nearest to the 50 % growth inhibition. Then, the other complexes such as Ni-ttpy IL, Cu-ttpy IL and Zn-ttpy IL exposed the control growth inhibition above 50 %. Conversely, the percentage control growth of IL tagged terpyridine complexes were compared with the positive control Adriamycin, in addition to that, Zn-ttpy IL complex explicit an excellent activity against HT-29 cell line. Nevertheless, the other IL terpyridine complexes were not shown superior activity than the control. Furthermore, the activity of complexes with cancer cell lines were further confirmed by fluorescent microscopic images. Microscopic observation manifested that after the incubation period of the cancer cells with IL tagged terpyridine complexes and control adriamycin underwent recognizable morphological transformation as exposed in Figs. 7–10. These remarkable changes indicated that the IL tagged terpyridine complexes can able to stimulate the adequate cell death on cancer cells in the tested cell lines [74].

Particularly, the cancer cells on treatment with positive control adriamycin also triggered to destroy the cells in HeLa (cervical), HT-29 (colon) and MCF-7 (breast) cancer cell lines. Hence, the microscopic images declared that the cells exhibiting cytological changes and further it undergoes the cell shrinkage prolonged to fragmentation of cells which may cause for the death of cancer cells [75]. Furthermore, IL tagged terpyridine complexes exhibiting their potential as dormant on MCF-7 breast cancer cell line but it possesses an impressive activity towards HeLa and HT-29 cell lines.

Overall performance of IL tagged terpyridine complexes established the anticancer activity of the zinc and copper complexes of terpyridine ILs were tightly bound with DNA through intercalation. Also, these complexes undergo DNA cleavage that leads to the existence of GSH (Glutathione) which yields H_2O_2 forming ROS (Reactive Oxygen Species). Hence, the function of GSH was decreased the level of oxygen in cancer cells. Meanwhile, these complexes were treated with cancer cells producing H_2O_2, this will promote the G0/G1 phase blocking along with programmed cell death (apoptosis or cellular suicide) [82].

The anticancer activity of IL tagged terpyridine complexes were scrutinized their role of resistance mechanism in accordance with the previously reported literature. Also, the obtained results especially, GI_{50} value of complexes and ionic liquids from recent literature was compared with the current IL tagged complexes (Table 4). In this scenario, our previous report viologen based dicationic ionic liquids showing an inhibitory action towards HeLa and HT-29 cancer cell lines less progressively than our current work [76]. Similarly, aldehyde encapsulated AgNps secures GI_{50} value as near to minimum concentration and exhibiting the anticancer potential [59]. In order to make strong evidence for the antitumor activity, the following stated

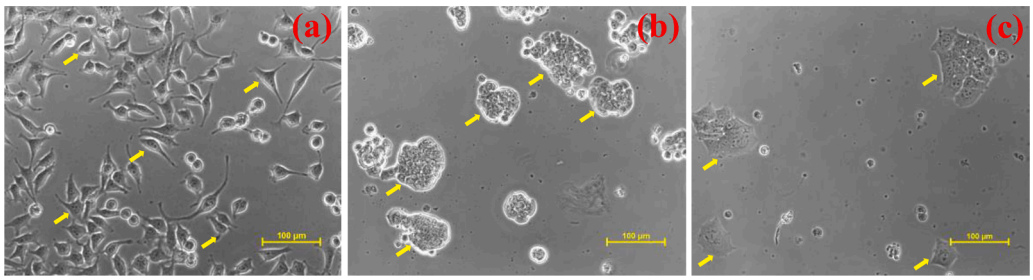

Fig. 7. Invitro anticancer activity photographs of untreated tumor cells (a) HeLa (cervical), (b) HT-29 (colon), (c) MCF-7 (breast) cancer cell lines. The yellow color arrow indicates an untreated tumor cell.

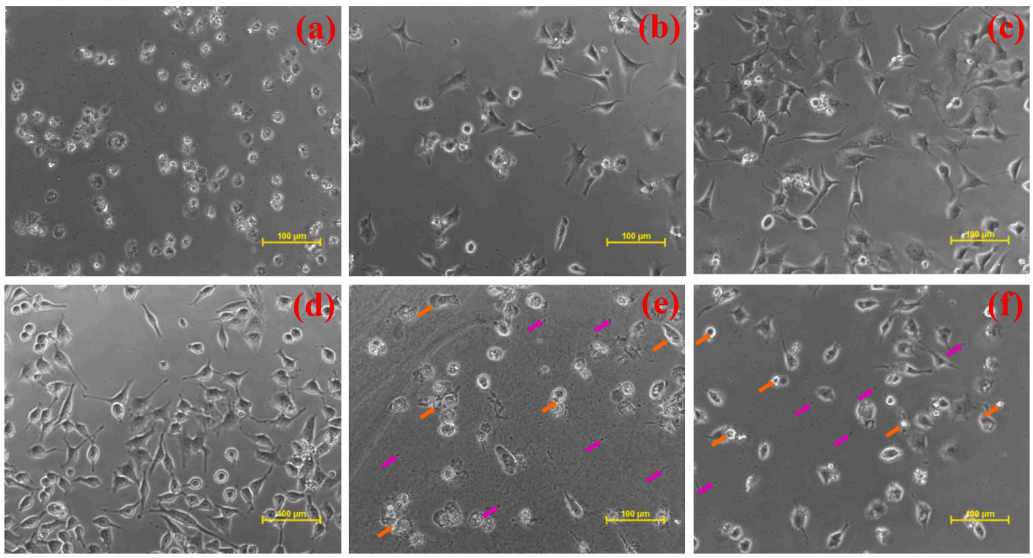

Fig. 8. Invitro anticancer activity photographs of (a) positive control, (b) Fe-ttpy-IL, (c) Co-ttpy-IL, (d) Ni-ttpy-IL, (e) Cu-ttpy-IL, (f) Zn-ttpy-IL viz., 80 μg/ml using HeLa cell line.

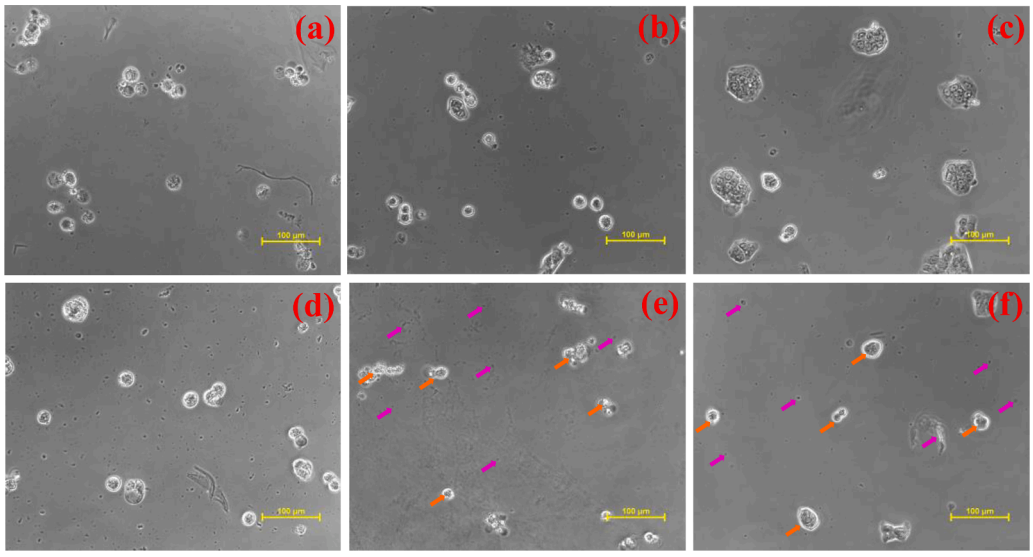

Fig. 9. Invitro anticancer activity photographs of (a) positive control, (b) Fe-ttpy-IL, (c) Co-ttpy-IL, (d) Ni-ttpy-IL, (e) Cu-ttpy-IL, (f) Zn-ttpy-IL i.e., 80 μg/ml using HT-29 tumor cell line. The pink arrow indicates the damaged HT-29 cells and an orange arrow indicate membrane blebbing.

compounds such as Dextran–Phenoxodiol [77], Violapyrones [78], 4-(4, 5-Diphenyl-1-(thiazol-2-yl)-1H-imidazol-2-yl)-2-meth-oxyphenol [79], C_{11}mimCl [80] and 5-(4-Chlorophenyl)-N-(4-fluorophenyl)-1,3,4-oxa-diazol-2- amine [81] revealed that the progression of anticancer activity was less as compared with the current GI_{50} value of IL-ttpy complexes (table 4). Notably, IL tagged terpyridine complexes reaches GI_{50} value with very low concentration than that were reported in literatures. Hence IL tagged terpyridine complexes were significantly considered as a superior drug than the other findings.

4. Conclusion

In summary, the novel terpyridine based IL attached ligand and five metal complexes were successfully synthesized and reported. These, complexes were analytically studied by UV-Visible, FT-IR, ^{1}H & ^{13}C NMR and High-resolution Mass spectroscopic data. Further, antibacterial, antioxidant and antiproliferative screening of the terpyridine complexes could be analyzed thoroughly. Moreover, iron terpyridine IL exhibiting marvelous activity against all selected microorganisms as compared with the reference. The antioxidant results suggest that Cu-ttpy-IL and Zn-ttpy-IL are very effective to inhibit the nitric oxide radicals due to its lower IC_{50} value. Then, the antiproliferative screening of IL tagged terpyridine complexes were established towards HeLa (cervical cancer), HT-29 (colon cancer) and MCF-7 (breast cancer) cell lines. The test reports revealed that Cu-ttpy-IL and Zn-ttpy-IL had shown excellent activity towards HeLa and HT-29 cell lines. Hence, the terpyridine ILs can be considered as potent antimicrobial, antioxidant and anticancer substitutes in drug inventions.

CRediT authorship contribution statement

M. Antilin Princela: Conceptualization, Writing – original draft, Data curation, Methodology. **B.T. Delma:** Formal analysis, Investigation. **S. Lizy Roselet:** Writing – original draft. **M. Shirly Treasa:** Validation, Visualization. **M. Jaya Brabha:** Methodology. **C. Isac Sobana Raj:** Supervision, Writing – review & editing.

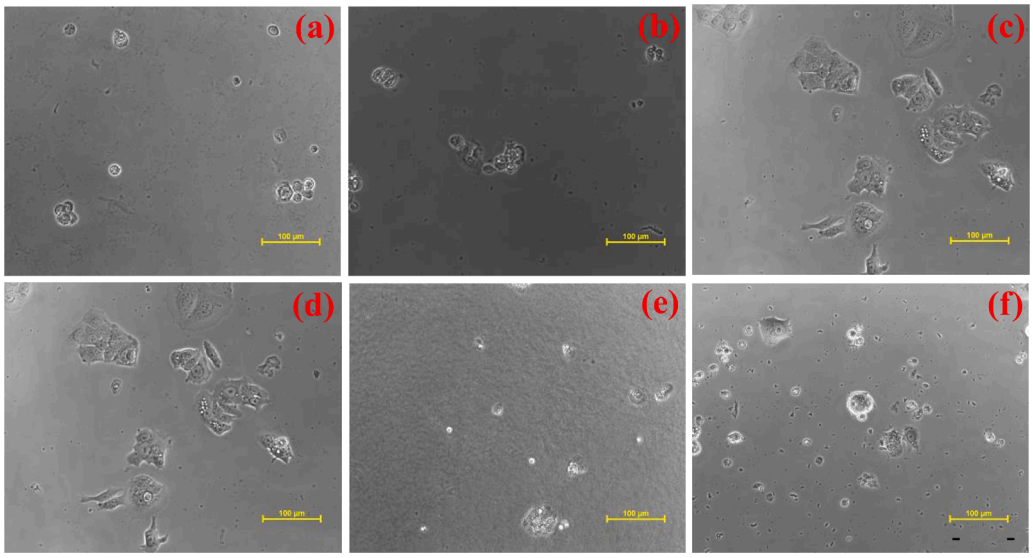

Fig. 10. Invitro anticancer activity photographic images of (a) positive control, (b) Fe-ttpy-IL, (c) Co-ttpy-IL, (d) Ni-ttpy-IL, (e) Cu-ttpy-IL, (f) Zn-ttpy-IL at 80 μg/ml using MCF-7 cell line.

Table 4
Comparable anticancer potential of Cu-ttpy IL and Zn-ttpy IL complexes to the recent reported compounds.

S. No	Name of the material	Cell line	GI_{50} value	Reference
1	Cu-ttpy IL, Zn-ttpy IL	(HeLa, HT-29)	<10 μM	Current work
2	$[2C_2$viologen$]$ $[BF_4]_2$	(HeLa, HT-29)	<10, 22 μM	[76]
3	A_{ald}–AgNPs	(MCF-7)	16.5 μM	[59]
4	Dextran–Phenoxodiol	(MRC-5)	26.7 μM	[77]
5	Violapyrones	(HeLa)	25.5 μM	[78]
6	4-(4,5-Diphenyl-1-(thiazol-2-yl)-1H-imidazol-2-yl)-2-meth-oxyphenol	(HeLa)	50 μM	[79]
7	C_{11}mimCl	NCI/ ADR-RES	55 μM	[80]
8	5-(4-Chlorophenyl)-N-(4-fluorophenyl)-1,3,4-oxadiazol-2-amine	(MCF-7)	24.5 μM	[81]

Declaration of Competing Interest

The authors declare that they have no known competing financial interests or personal relationships that could have appeared to influence the work reported in this paper.

Data availability

The data that has been used is confidential.

Supplementary materials

Supplementary material associated with this article can be found, in the online version, at doi:10.1016/j.chphi.2023.100371.

References

[1] Yi Lu, Steven M. Berry, Thomas D. Pfister, Engineering novel metalloproteins: design of metal-binding sites into native protein scaffolds, Chem/ Rev/ 101 (2001) 3047–3080.
[2] C.I.R. Sobana, G.A.R. Gnana, M.A. Princela, Synthesis and characterization of bioactive transition metal complexes of Zr (IV) and (IV) using di-α-formylmethoxy bis (3-penta decenyl phenyl) methane (DFMPM) derived from Cardanol, AJCPR: Asian J.Chem. Pharmaceut/ Res/ 3 (2015) 208–214.
[3] Andreas Buhr, Roland Baur, Erwin Sigel, Subtle changes in residue 77 of the γ subunit of α1β2γ2 GABAA receptors drastically alter the affinity for ligands of the benzodiazepine binding site, J. Biolog.Chem. 272 (1997) 11799–11804.
[4] Meng Zhao, et al., Insights into metalloenzyme microenvironments: biomimetic metal complexes with a functional second coordination sphere, Chem. Soc. Rev. 42 (2013) 8360–8375.
[5] C. Raj, C.M. Sofia, M.Antilin Princela, Synthesis and Characterization of Bioactive Transition Metal Complexes from Cardanol, Asian J. Res. Chem. 7 (2014) 711–716.
[6] Attila Kovacs, Gernot Frenking, Stability and Bonding Situation of Electron-Deficient Transition-Metal Complexes. Theoretical Study of the CO-Labilizing Effect of Ligands L in $[W(CO)_5L]$ (L= C_2H_2, NCH, N_2, C_2H_4, OH_2, SH_2, NH_3, F^-, Cl^-, OH^-, SH^-) and $[W(CO)_4L]^{2-}$ (L^{2-}= $O_2C_2H_2^{2-}$, $S_2C_2H_2^{2-}$) and the Structure of the 16-Valence-Electron Complexes $[W(CO)_4L]$ and $[W(CO)_3L]^{2-}$, Organometallics 20 (2001) 2510–2524.
[7] Naoya Shibayama, Allosteric transitions in hemoglobin revisited, Biochimica et Biophys. Acta (BBA)-Gen. Sub. 1864 (2020), 129335.
[8] Sergey V Dorozhkin, Bioceramics of calcium orthophosphates, Biomaterials 31 (2010) 1465–1485.
[9] Giovanni Floris, et al., The physiopathological significance of ceruloplasmin: a possible therapeutic approach, Biochem. Pharmacol. 60 (2000) 1735–1741.
[10] Deenah Osman, et al., The requirement for cobalt in vitamin B12: A paradigm for protein metalation, Biochim. Biophys. Acta (BBA)-Mol. Cell Res. 1868 (2021), 118896.
[11] Jodi L. Boer, Scott B. Mulrooney, Robert P. Hausinger, Nickel-dependent metalloenzymes, Arc Biochem. Biophys. 544 (2014) 142–152.
[12] Alexandra Vardi Kilshtain, Arieh Warshel, On the origin of the catalytic power of carboxypeptidase A and other metalloenzymes, Proteins: Struct, Function, Bioinf. 77 (2009) 536–550.
[13] Harald Hofmeier, Ulrich S. Schubert, Recent developments in the supramolecular chemistry of terpyridine–metal complexes, Chem. Soc. Rev. 33 (2004) 373–399.
[14] Kai Wing Cheng, et al., Synthesis of conjugated polymers with pendant ruthenium terpyridine trithiocyanato complexes and their applications in heterojunction photovoltaic cells, J. Poly. Sci. Part A: Poly. Chem. 46 (2008) 1305–1317.
[15] M.Concepción Gimeno, et al., Synthesis, photochemical, and redox properties of gold (I) and gold (III) pincer complexes incorporating a 2, 2′: 6′, 2 ″-terpyridine ligand framework, Inorgan. Chem. 54 (2015) 10667–10677.
[16] Aaron Breivogel, Christoph Kreitner, Katja Heinze, Redox and photochemistry of bis (terpyridine) ruthenium (II) amino acids and their amide conjugates–from understanding to applications, Eur. J. Inorganic Chem. 2014 (2014) 5468–5490.
[17] Dawid Pakulski, et al., High-sorption terpyridine–graphene oxide hybrid for the efficient removal of heavy metal ions from wastewater, Nanoscale 13 (2021) 10490–10499.
[18] Ding Zhou, et al., Graphene–terpyridine complex hybrid porous material for carbon dioxide adsorption, Carbon 66 (2014) 592–598.
[19] Hironobu Ozawa, et al., Highly efficient dye-sensitized solar cells based on a ruthenium sensitizer bearing a hexylthiophene modified terpyridine ligand, J. Mater. Chem. A 4 (2016) 1762–1770.
[20] Paolo Salvatori, et al., A new terpyridine cobalt complex redox shuttle for dye-sensitized solar cells, Inorgan. Chimica Acta 406 (2013) 106–112.

[21] Guoqi Zhang, Shengping Zheng, Michelle C. Neary, An ionic Fe-based metal–organic-framework with 4′-pyridyl-2, 2′: 6′, 2″-terpyridine for catalytic hydroboration of alkynes, RSC Adv. 13 (2023) 2225–2232.
[22] Yuxuan Liu, et al., Rhodium-terpyridine catalyzed redox-neutral depolymerization of lignin in water, Green Chem. 22 (2020) 33–38.
[23] Meiheng Lu, et al., Theoretical insights into the sensing mechanism of a series of terpyridine-based chemosensors for TNP, Chem. Phys. Letters 725 (2019) 45–51.
[24] Rui Rui Zhao, et al., A coumarin-based terpyridine–zinc complex for sensing pyrophosphate and its application in in vivo imaging, Tetrahedron Lett. 57 (2016) 5022–5025.
[25] Ibrahim Eryazici, Charles N. Moorefield, George R. Newkome, Square-planar Pd (II), Pt (II), and Au (III) terpyridine complexes: their syntheses, physical properties, supramolecular constructs, and biomedical activities, Chem. Rev. 108 (2008) 1834–1895.
[26] Hui Wang, et al., Synthesis, crystal structure, photophysical property and bioimaging application of a series of Zn (II) terpyridine complexes, J. M. Struct. 1194 (2019) 157–162.
[27] Simon Cerfontaine, et al., Efficient Convergent Energy Transfer in a Stereoisomerically Pure Heptanuclear Luminescent Terpyridine-Based Ru (II)–Os (II) Dendrimer, Inorgan. Chem. 59 (2020) 14536–14543.
[28] Badri Zaman Momeni, et al., Crystal exploring, Hirshfeld surface analysis, and properties of 4′-(furan-2-yl)-2, 2′: 6′, 2 ″-terpyridine complexes of nickel (II): New precursors for the synthesis of nanoparticles, Appl. Organometall. Chem. 35 (2021) 6179.
[29] Andreas Winter, et al., The marriage of terpyridines and inorganic nanoparticles: synthetic aspects, characterization techniques, and potential applications, Adv. Mater. 23 (2011) 5728–5748.
[30] Tripti Mandal, et al., Terpyridine derivatives as “turn-on” fluorescence chemosensors for the selective and sensitive detection of Zn^{2+} ions in solution and in live cells, Photochem. Photobiol. Sci. 17 (2018) 1068–1074.
[31] Rahul Kaushik, Amrita Ghosh, D.Amilan Jose, Simple terpyridine based Cu (II)/Zn (II) complexes for the selective fluorescent detection of H_2S in aqueous medium, J. Luminesce. 171 (2016) 112–117.
[32] Sebastian Amthor, et al., Strong ligand stabilization based on π-extension in a series of ruthenium terpyridine water oxidation catalysts, Chem.–A Eur. J. 27 (2021) 16871–16878.
[33] Jane J. Leung, et al., Solar-driven reduction of aqueous CO_2 with a cobalt bis (terpyridine)-based photocathode, Nat. Catal. 2 (2019) 354–365.
[34] Long-Xuan Zhao, et al., Synthesis, topoisomerase I inhibition and antitumor cytotoxicity of 2, 2′: 6′, 2 ″-, 2, 2′: 6′, 3 ″-and 2, 2′: 6′, 4 ″-Terpyridine derivatives, Bioorgan. Med. Chem. Lett. 11 (2001) 2659–2662.
[35] Franck Camerel, et al., Formation of Gels and Liquid Crystals Induced by Pt··· Pt and p–p* Interactions in Luminescent s-Alkynyl Platinum (II) Terpyridine Complexes, Angew. Chem. Int. Ed. 46 (2007) 2659–2662.
[36] Chaoyang Li, et al., Platinum (II) terpyridine anticancer complexes possessing multiple mode of DNA interaction and EGFR inhibiting activity, Front. Chem. 8 (2020) 210.
[37] T. Ezhilarasu, S. Balasubramanian, Synthesis, Characterization, Photophysical and Electrochemical Studies of Ruthenium (II) Complexes with 4′-Substituted Terpyridine Ligands and Their Biological Applications, ChemistrySelect 3 (43) (2018) 12039–12049.
[38] J.W. Liang, Y. Wang, K.J. Du, G.Y. Li, R.L. Guan, L.N. Ji, H. Chao, Synthesis, DNA interaction and anticancer activity of copper (II) complexes with 4′-phenyl-2, 2′: 6′, 2 ″-terpyridine derivatives, J. Inorgan. Biochem. 141 (2014) 17–27.
[39] X. Wang, R. Li, A. Liu, C. Yue, S. Wang, J. Cheng, J. Li, Z. Liu, Syntheses, crystal structures, antibacterial activities of Cu (II) and Ni (II) complexes based on terpyridine polycarboxylic acid ligand, J. Mol. Struct. 1184 (2019) 503–511.
[40] K. Velugula, A. Kumar, J.P. Chinta, Nuclease and anticancer activity of antioxidant conjugated terpyridine metal complexes, Inorgan. Chimica Acta 507 (2020), 119596.
[41] Z. Naseri, A.N. Kharat, A. Banavand, A. Bakhoda, S. Foroutannejad, First row transition metal complexes of thienyl substituted terpyridine: structural, photophysical and biological studies, Polyhedron 33 (1) (2012) 396–403.
[42] C.I. Sobanaraj, M.A. Princela, Efficiency of Salen Functionalized Ionic Liquids and their Application towards Biological Activity, Int. J. Pharmaceut. Sci. Nanotechnol. (IJPSN) 13 (4) (2020) 5020–5027.
[43] I. Ali, M. Suhail, M. Locatelli, S. Ali, Y. Aboul-Enein H., Role of Ionic Liquids in Capillary Electrophoresis, Analytica 3 (2) (2022) 236–250.
[44] I. Ali, Z.A. Alothman, A. Alwarthan, H.Y. Aboul-Enein, Applications of ionic liquids in chemical science, Novel Dev. Pharmaceut. Biomed. Anal. 2 (2018) 382–412.
[45] A. Hussain, M.F. AlAjmi, I. Hussain, I. Ali, Future of ionic liquids for chiral separations in high-performance liquid chromatography and capillary electrophoresis, Crit. Rev. Anal. Chem. 49 (4) (2019) 289–305.
[46] I. Ali, G.T. Imanova, H.M. Albishri, W.H. Alshitari, M. Locatelli, M.N. Siddiqui, A. M. Hameed, An ionic-liquid-imprinted nanocomposite adsorbent: Simulation, kinetics and thermodynamic studies of triclosan endocrine disturbing water contaminant removal, Molecules 27 (17) (2022) 5358.
[47] I. Ali, M. Suhail, M.M. Sanagi, H.Y. Aboul-Enein, Ionic liquids in HPLC and CE: a hope for future, Crit. Rev. Anal. Chem. 47 (4) (2017) 332–339.
[48] I. Ali, Z.A. Alothman, A. Alwarthan, Uptake of propranolol on ionic liquid iron nanocomposite adsorbent: kinetic, thermodynamics and mechanism of adsorption, J. Mol. Liquids 236 (2017) 205–213.
[49] I. Ali, S. Afshinb, Y. Poureshgh, A. Azari, Y. Rashtbari, A. Feizizadeh, A. Hamzezadeh, M. Fazlzadeh, Green preparation of activated carbon from pomegranate peel coated with zero-valent iron nanoparticles (nZVI) and isotherm and kinetic studies of amoxicillin removal in water, Environ. Sci. Poll. Res. 27 (2020) 36732–36743.
[50] I. Ali, I. Burakova, E. Galunin, A. Burakov, E. Mkrtchyan, A. Melezhik, D. Kurnosov, A. Tkachev, V. Grachev, High-speed and high-capacity removal of methyl orange and malachite green in water using newly developed mesoporous carbon: kinetic and isotherm studies, ACS Omega 4 (21) (2019) 19293–19306.
[51] I. Ali, A.V. Babkin, I.V. Burakova, A.E. Burakov, E.A. Neskoromnaya, A.G. Tkachev, S. Panglisch, N. AlMasoud, T.S. Alomar, Fast removal of samarium ions in water on highly efficient nanocomposite-based graphene oxide modified with polyhydroquinone: Isotherms, kinetics, thermodynamics and desorption, J. Mol. Liquids 329 (2021), 115584.
[52] I. Ali, T. Kon’kova, V. Kasianov, A. Rysev, S. Panglisch, X.Y. Mbianda, M.A. Habila, N. AlMasoud, Preparation and characterization of nano-structured modified montmorillonite for dioxidine antibacterial drug removal in water, J. Mol. Liquids 331 (2021), 115770.
[53] Rahman Md Moshikur, et al., Biocompatible ionic liquids and their applications in pharmaceutics, Green Chem. 22 (2020) 8116–8139.
[54] A.W. Bauer, Antibiotic susceptibility testing by a standardized single diffusion method, Am. J. Clin. Pathol. 45 (1966) 493–496.
[55] Pilar Prieto, Manuel Pineda, Miguel Aguilar, Spectrophotometric quantitation of antioxidant capacity through the formation of a phosphomolybdenum complex: specific application to the determination of vitamin E, Anal. Biochem. 269 (1999) 337–341.
[56] M.N.A. Rao, Nitric oxide scavenging by curcuminoids, J. Phar. Pharmacol. 49 (1997) 105–107.
[57] Sunil Kumar, et al., Antioxidant and free radical scavenging potential of Citrullus colocynthis (L.) Schrad. methanolic fruit extract, Acta Pharmaceut. 58 (2008) 215–220.
[58] Philip Skehan, et al., New colorimetric cytotoxicity assay for anticancer-drug screening, JNCI: J. Natl. Cancer Inst. 82 (1990) 1107–1112.
[59] F. Kholiya, S. Chatterjee, G. Bhojani, S. Sen, M. Barkume, N.K. Kasinathan, J. Kode, R. Meena, Seaweed polysaccharide derived bioaldehyde nanocomposite: Potential application in anticancer therapeutics, Carbohyd. Poly. 240 (2020), 116282.
[60] Pauline L. Bellavance, et al., Synthesis and characterization of complexes of aluminum halide with 2, 2′-bipyridine, 1, 10-phenanthroline and 2, 2′, 2″-terpyridine in acetonitrile, Inorgan. Chem. 16 (1977) 462–467.
[61] Biswajit Sinha, Malay Bhattacharya, Sanjoy Saha, Transition metal complexes obtained from an ionic liquid-supported Schiff base: synthesis, physicochemical characterization and exploration of antimicrobial activities, J. Chem. Sci. 131 (2019) 1–10.
[62] R.K. Parashar, et al., Stability studies in relation to IR data of some schiff base complexes of transition metals and their biological and pharmacological studies, Inorgan. Chimica Acta 151 (1988) 201–208.
[63] Robert M. Berger, David R. McMillin, Ultraviolet and visible resonance raman spectroscopy of tris-(2, 2′-bipyridyl) iron (II): intensity considerations and band assignments, Inorgan. Chimica Acta 177 (1990) 65–69.
[64] Ibrahim Eryazici, Charles N. Moorefield, George R. Newkome, Square-planar Pd (II), Pt (II), and Au (III) terpyridine complexes: their syntheses, physical properties, supramolecular constructs, and biomedical activities, Chem. Rev. 108 (2008) 1834–1895.
[65] Zhen Ma, et al., Inorgan. Biochem. 104 (2010) 704–711.
[66] Thiravidamani Chandrasekar, Narayanaperumal Pravin, Natarajan Raman, Biosensitive metal chelates from curcumin analogues: DNA unwinding and anti-microbial evaluation, Inor. Chem. Commun. 43 (2014) 45–50.
[67] E.U. Mughal, M. Mirzaei, A. Sadiq, S. Fatima, A. Naseem, N. Naeem, N. Fatima, S. Kausar, A.A. Altaf, M.N. Zafar, B.A. Khan, Terpyridine-metal complexes: effects of different substituents on their physico-chemical properties and density functional theory studies, Royal Soc. Open Sci. 7 (11) (2020), 201208.
[68] M.S.S. Adam, Zn (II)-complexes of diisatin dihydrazones as effective catalysts in the oxidation protocol of benzyl alcohol and effective reagents for biological studies, J. Mol. Liquids 381 (2023), 121841.
[69] E. Selimović, S. Jeremić, B. Ličina, T. Soldatović, Kinetics, DFT study and antibacterial activity of zinc (II) and copper (II) terpyridine complexes, J. Mexican Chem. Soc. 62 (1) (2018).
[70] M. Mondelli, V. Bruné, G. Borthagaray, J. Ellena, O.R. Nascimento, C.Q. Leite, A. A. Batista, M.H. Torre, New Ni (II)-sulfonamide complexes: Synthesis, structural characterization and antibacterial properties. X-ray diffraction of [Ni (sulfisoxazole) 2 (H_2O) 4]· 2H_2O and [Ni (sulfapyridine)$_2$], J. Inor. Biochem. 102 (2) (2008) 285–292.
[71] M.S.S. Adam, A.M. Abu-Dief, M.M. Makhlouf, S. Shaaban, S.O. Alzahrani, F. Alkhatib, G.S. Masaret, M.A. Mohamed, M. Alsehli, N.M. El-Metwaly, A.D. M. Mohamad, Tailoring, structural inspection of novel oxy and non-oxy metal-imine chelates for DNA interaction, pharmaceutical and molecular docking studies, Polyhedron 201 (2021), 115167.
[72] G. Martemucci, C. Costagliola, M. Mariano, L. D’andrea, P. Napolitano, A. G. D’Alessandro, Free radical properties, source and targets, antioxidant consumption and health, Oxygen 2 (2) (2022) 48–78.
[73] E. Lubos, D.E. Handy, J. Loscalzo, Role of oxidative stress and nitric oxide in atherothrombosis, Front. Biosci.:J. virtual Libr. 13 (2008) 5323.
[74] M.J.A. Abualreish, A.D.M. Mohamad, M.S.S. Adam, Comprehensive catalytic and biological studies on new designed oxo-and dioxo-metal (IV/VI) organic arylhydrazone frameworks, J. Mol. Liq.uid 375 (2023), 121309.
[75] M.S.S. Adam, H. Elsawy, A. Sedky, M.M. Makhlouf, A. Taha, Catalytic potential of sustainable dinuclear (Cu^{2+} and ZrO^{2+}) metal organic incorporated frameworks with comprehensive biological studies, J.Taiwan Inst.Chem. Eng. 144 (2023), 104747.

[76] C.I. Sobanaraj, M.A. Princela, Invitro Screening of dicationic ionic liquids and their consequence towards biological strategies, *Int. J. Sci. Technol. Res.* (IJSTR) 8 (9) (2020) 2189–2198.
[77] E.M. Yee, G. Cirillo, M.B. Brandl, D.S. Black, O. Vittorio, N. Kumar, Synthesis of dextran–phenoxodiol and evaluation of its physical stability and biological activity, Front. Bioeng. Biotechnol. 7 (2019) 183.
[78] H.J. Shin, H.S. Lee, J.S. Lee, J. Shin, M.A. Lee, H.S. Lee, Y.J. Lee, J. Yun, J.S. Kang, Violapyrones H and I, new cytotoxic compounds isolated from Streptomyces sp. associated with the marine starfish Acanthaster planci, Marine Drugs 12 (6) (2014) 3283–3291.
[79] A.P.G. Nikalje, S.V. Tiwari, A.P. Sarkate, K.S. Karnik, Imidazole-thiazole coupled derivatives as novel lanosterol 14-α demethylase inhibitors: Ionic liquid mediated synthesis, biological evaluation and molecular docking study, Med. Chem. Res 27 (2018) 592–606.
[80] S.V. Malhotra, V. Kumar, A profile of the in vitro anti-tumor activity of imidazolium-based ionic liquids, Bioorg. Med. Chem. Lett. 20 (2) (2010) 581–585.
[81] M. Agarwal, V. Singh, S.K. Sharma, P. Sharma, M.Y. Ansari, S.S. Jadav, S. Yasmin, R. Sreenivasulu, M.Z. Hassan, V. Saini, M.J. Ahsan, Design and synthesis of new 2, 5-disubstituted-1, 3, 4-oxadiazole analogues as anticancer agents, Med. Chem. Res. 25 (2016) 2289–2303.
[82] M.M. Liu, R.H. Ma, Z.J. Ni, K. Thakur, C.L. Cespedes-Acuña, L. Jiang, Z.J. Wei, Apigenin 7-O-glucoside promotes cell apoptosis through the PTEN/PI3K/AKT pathway and inhibits cell migration in cervical cancer HeLa cells, Food Chem. Toxicol. 146 (2020), 111843.